The impact of canopy geometry on particle dispersion gradients in sparse agricultural canopies

Brian N. Bailey

University of Utah, Salt Lake City, Utah

R. Stoll

University of Utah, Salt Lake City, Utah

W. Mahaffee

USDA ARS, Corvalis, Oregon

E. Pardyjak

University of Utah, Salt Lake City, Utah

ABSTRACT

Turbulent dispersion is one of the most important transport mechanisms in the life cycle of many fungal plant pathogens. Without turbulent dispersion both inoculum spread beyond leaves adjacent to infection sites and epidemics would be limited in severity. Thus, understanding the mechanisms that influence and control dispersion gradients from disease foci are of primary importance towards improving our ability to prevent and respond to disease outbreaks. In sparse canopy environments, the influence of canopy geometry (row spacing, canopy height, and plant density) on turbulent fluxes results in highly intermittent transport. This can be problematic for traditional dispersion modeling techniques that rely on assumptions of steady or horizontally homogeneous velocity fields. Here, the link between canopy geometry, turbulent fluxes and particle dispersion gradients in sparse agricultural canopies is explored using a Lagrangian particle dispersion model linked to velocity fields from large-eddy simulations. In particular, particle dispersion from point and line sources in plant canopies with geometry characteristic of grape vineyards are examined. Simulations are performed with varying row spacing, canopy height and particle source height to characterize the length and velocity scales associated with turbulent fluxes and particle dispersion gradients within the canopy.

1. Introduction

Plant disease outbreaks caused by airborne pathogens present a substantial hazard to vegetative growth. Outbreaks can be detrimental economically and impact the security of the food supply (Agrios, 2005). In this research, our interest is focused on transport of

Erysiphe necetor (powdery mildew of Vitis vinifera L., grapes) spores in grape vineyards. Turbulent wind transport is the primary mechanism by which E. necetor and most other fungal spores are spread (Aylor, 1999). The epidemic severity of diseases caused by these fungal pathogens is strongly linked to the distance and speed that spores can travel from initial sources of inoculum. Therefore, understanding turbulent transport of spores is of primary importance toward understanding fungal plant disease epidemiology (McCartney et al., 2006). This makes understanding the mechanisms that influence and control dispersion gradients from disease foci of great importance towards improving our ability to prevent and respond to disease outbreaks.

For perinnial plants like grape vines, the existance of the plant canopy has a strong impact on turbulent fluxes (Finnigan, 2000) and presumably on spore transport through the canopy. While a strong understanding of how continuous canopies impact turbulent transport processes and flow structures has started to develop (e.g., Finnigan et al., 2009), the same can not be said of discontinuous canopies where a substantial percentage of the canopy is open. Motivated by the importance of turbulent transport in epidemic development and by the sparse nature of most vineyards, we examine how plant canopy geometry (row spacing, canopy height and plant density) interacts with atmospheric flow characteristics to impact the dispersion of airborne plant pathogen spores in grape vineyards using a computational model.

2. Vineyard Canopy Simulation

Numerical simulation of the turbulent ABL was performed using large-eddy simulation (LES), in which the filtered Navier-Stokes equations were solved within and above the plant canopy. The sub-filter scale stress term was modeled using a scale-dependent dynamic Smagorinsky model (Stoll et al., 2006). The presence of the canopy was represented as a local drag force term that was added to the right-hand side of the governing momentum equations. This term was calculated as follows:

$$F_i = c_d \, a \, \widetilde{u_i} \, \widetilde{V}, \tag{1}$$

where c_d is the drag coefficient, a is the local leaf area density (equal to zero in areas of no vegetation), $\tilde{u_i}$ is the filtered velocity component, and $\tilde{V}$ is the filtered velocity magnitude.

In traditional simulations, agricultural canopies are treated as a horizontally homogeneous volumes of vegetation, where the spaces between vegetation are not explicitly resolved (Shaw et al. 1992, Patton et al. 1998, Aylor et al. 2001). Here, because of the emphasis on the impact of canopy geometry, we performed LES of vineyard canopies where the canopy row structure is resolved.

The spore particles were modeled as passive fluid parcels whose positions were calculated according to the equation:

$$\frac{dx_i}{dt} = \widetilde{u_i} + u_i'. \tag{2}$$

The sub-filter velocity (u_i') is not known and was modeled as a Gaussian random number scaled by the resolved velocity variance (Uliasz, 1994.) The vertical component (u_3') inclued

an additional term to account for the settling of particles due to gravity. The drift velocity used in the settling term was constant for all particles, and therefore did not inclue any size distribution among particles. A stochastic model was used to determine the probability that particles within the canopy would be deposited onto plant foliage (Aylor et al., 2001). A similar model was used to determine whether particles that hit the ground would either ricochet upward, or become deposited.

a. Effect of Canopy Geometry on Particle Dispersion

Ten simulations were run in which the leaf area index (LAI) of individual rows (exluding open spaces) and the row spacing of the vineyard were varied. An approximately 18x18x6 m^3 volume was simulated with a horizontal resolution of 0.18 m and a vertical resolution of 0.10 m. Cases were run for row spacings of 1, 1.5, 2, 2.5, and 3 meters for LAI values of 1 and 3. This range of values represent the typical variability observed in actual vineyards (Johnson et al., 2003). In each case, the volume average of the streamwise velocity was held at a constant value of 2 m/s. Furthermore, the shape of the leaf area density profile in each case was held constant, and was simply scaled to achieve integrated LAI values of 1 and 3.

3. Results

Near source particle distributions were examined to determine how spores spread in the vicinity of the source. Figure 1 shows concentration contours averaged in the spanwise direction for a simulation with a LAI of 3 and row spacing of 2 meters. As the particles

approach a row, many of the particles are either deflected up and out of the canopy, or down into the trunk space. A large percentage of the particles which travel into the foliage of the row are deposited, resulting in the low concentration area observed in the wake of the foliage. For sufficiently large row spacing, some particles above the canopy are swept back into the canopy, and the process is repeated for each row.

To examine the impact of changing row spacing and LAI, particle concentration profiles are shown in Figure 2 for a downstream location of 8 m. The results indicate that as LAI is increased, downstream particle concentration tends to decrease in general. Furthermore, as row spacing is decreased, downstream particle concentration tends to also decrease.

Long distance particle transport was also of interest because of its importance in determining epidemic velocity (Mundt et al., 2009). To examine long distance particle transport, an instantaneous puff of particles were released and tracked over a specified period of time. The probability density function of how far particles traveled over the specified time period was calculated for each vineyard geometry case. Results (not shown) indicate that increasing LAI or decreasing row spacing tended to reduce the probability of long-range particle transport.

Acknowledgments.

B. N. Bailey and R. Stoll gratefully acknowledge support from a University of Utah research foundation SEED grant. Computational resources were provided by the University of Utah Center for High Performance Computing.

REFERENCES

Agrios, G., 2005: *Plant Pathology*. New York: Elsevier Academic Press.

Aylor, D. E., 1999: Biophysical scaling and the passive dispersal of fungus spores: relationship to integrated pest management strategies. *Agric. For. Meteorol.*, **97**, 275–292.

Aylor, D. E., 2003: Spread of plant disease on a continental scale: Role of aerial dispersal of pathogens. *Ecology*, **84**, 215–219.

Aylor, D. E. and T. K. Flesch, 2001: Estimating spore release rates using a lagrangian stochastic simulation model. *Journal of Applied Meteorology*, **40**, 1196–1208.

Finnigan, J. J., 2000: Turbulence in plant canopies. *Ann. Rev. Fluid Mech.*, **32**, 519–571.

Finnigan, J. J., R. H. Shaw, and E. G. Patton, 2009: Turbulence structure above a vegetation canopy. *Journal of Fluid Mech.*, **637**, 387–424.

Johnson, L. F., D. E. Roczen, S. K. Youkhana, R. R. Nemani, and D. F. Bosch, 2003: Mapping vineyard leaf area with multispectral satellite imagery. *Comp. and Elec. in Agric.*, **38**, 33–44.

McCartney, H. A., B. D. L. Fitt, and J. S. West, 2006: Dispersal of foliar plant pathogens. *The Epidemiology of Plant Diseases*, B. M. Cooke, D. G. Jones, and B. Kaye, Eds., Springer, 159–192.

Mundt, C. C., 2009: Importance of autoinfeciton to the epidemiology of polycyclic foliar disease. *Phytopathology*, **99**, 1116–1120.

Patton, E. G., R. H. Shaw, M. J. Judd, and M. R. Raupach, 1998: Large-eddy simulation of windbreak flow. *Boundary-Layer Meteor.*, **87**, 275–307.

Shaw, R. H. and U. Schumann, 1992: Large-eddy simulation of turbulent flow above and within a forest. *Boundary-Layer Meteor.*, **61**, 47–64.

Stoll, R. and F. Porté-Agel, 2006: Dynamic subgrid-scale models for momentum and scalar fluxes in large-eddy simulations of neutrally stratified atmospheric boundary layers over heterogeneous terrain. *Water Resour. Res.*, **42**, W01 409.

Uliasz, M., 1994: Lagrangian particle dispersion modeling in mesoscale applications. *Environmental Modeling - Vol. II*, 71–101.

List of Figures

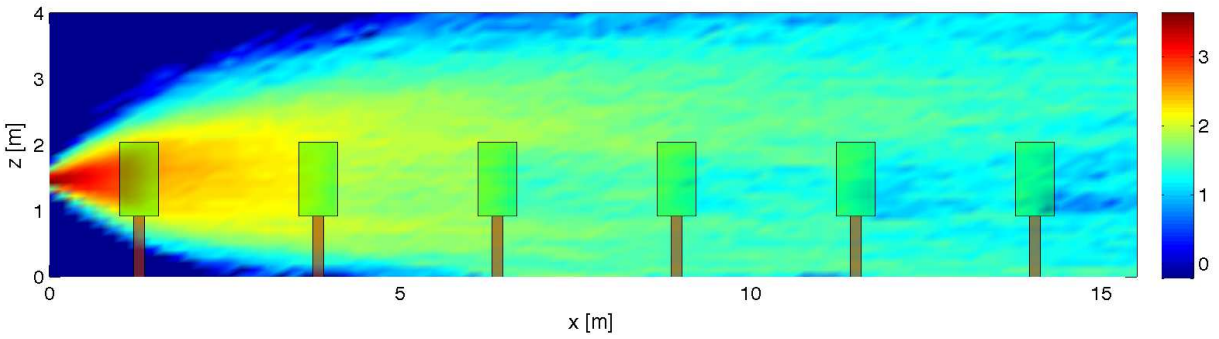

FIG. 1. Contours of particle concentration averaged in the streamwise direction for an LAI of 3 and row spacing of 2 meters

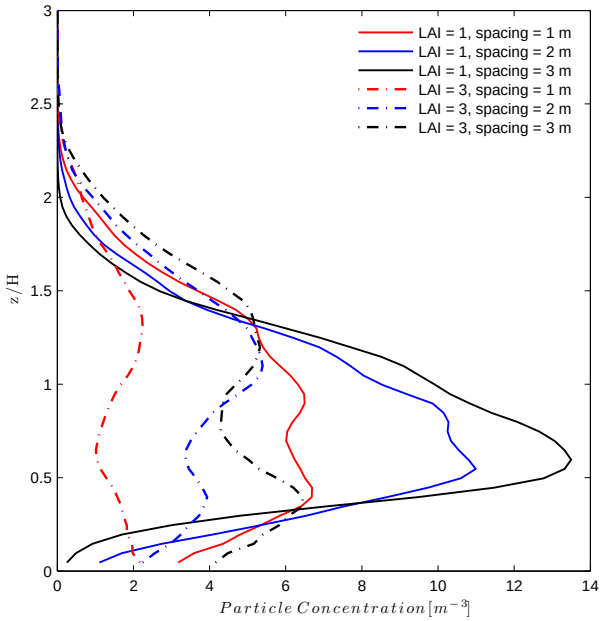

FIG. 2. Particle concentration profiles at 8 m downstream of the release point